Applied Composite Materials **2:** 293–311, 1995.

A Nondestructive Approach to Correlate the Interfacial Defects Induced During Processing of MMCs and CMCs with the Consolidation Parameters*

THEODORE E. MATIKAS and PRASANNA KARPUR
Research Institute, University of Dayton, 300 College Park Avenue, Dayton, OH 45469-0127, USA

S. KRISHNAMURTHY
UES, Inc., Dayton, OH USA

ROLLIE E. DUTTON
NIST, Materials Directorate, Wright Laboratory, Wright-Patterson Air Force Base, OH 45433, USA

(Received 29 August 1995; accepted 12 September 1995)

Abstract. An ultrasonic nondestructive methodology for evaluating the consolidation and microstructure of advanced fiber-reinforced composites has been developed to aid in their design and fabrication. The use of this nondestructive evaluation (NDE) technique can enable optimization of the processing parameters to obtain complete densification around the fibers. In addition, the methodology can be used to ensure that the composite panels are devoid of any global problems such as fiber swimming, ply delamination, embedded manufacturing anomalies such as voids, etc. Such a post processing NDE is also essential before any interfacial characterization is performed. The technique described in this paper, being generic, is applicable to both metal matrix and ceramic matrix composites.

Key words: ultrasound, metal matrix composite, ceramic matrix composite, consolidation, processing parameters, nondestructive evaluation.

1. Introduction

Ultrasonic NDE techniques have been used in the past for global inspection of composites to determine the distribution of reinforcements and detecting the defects present in composite panels [1]. In the case of fiber-reinforced metal matrix composites, ultrasonic methods have been employed to screen for macroscopic defects such as ply delaminations and nonuniform fiber spacing arising from either missing fibers or displacement of fibers during fabrication [1, 2].

* This work was supported by and performed on-site in the Materials Directorate, Wright Laboratory, Materiel Command, Wright-Patterson Air Force Base, Ohio, USA. Contract nos. F33615-94-C-5213 (T. E. Matikas and P. Karpur), F33615-91-C-5663 (S. Krishnamurthy).

The ultrasonic approach here provides a method to assess the consolidation on a 'microscopic' or localized level, and is a quick and reliable tool for post-processing evaluation of the consolidation of advanced composites.

Composites based on reactive matrices with high melting temperatures such as titanium alloys are usually processed by solid state diffusion bonding of matrix foils, powders, or sprayed deposits with reinforcements [3]. For example, the processing of continuously reinforced titanium matrix composites by the foil-fiber-foil method typically involves diffusion bonding of rolled matrix alloy foils with reinforcing fibers in the form of woven mats with a cross-weave to hold the fibers in place [4]. The foils and the fiber mats are stacked alternately and consolidated by vacuum hot pressing or hot isostatic pressing. The processing conditions are carefully selected in order to achieve complete consolidation and produce acceptable composite material. While higher temperatures and longer processing times may enable consolidation, they can promote undesirable reactions at the fiber/matrix interface and also cause high residual stresses after the composite is cooled to ambient temperature. On the other hand, lower processing temperatures can lead to fiber damage as well as incomplete consolidation. In practice, optimum processing conditions are determined through preliminary diffusion bonding experiments. The initial processing temperatures are chosen on the basis of known flow characteristics of the matrix alloy at different temperatures and strain rates, and the consolidation of these samples is checked by metallographic examination of polished sections. However, the use of metallography alone is tedious and generally inadequate since consolidation often occurs nonuniformly within the composite panels.

Similar to MMCs, densification problems are also encountered in the fabrication of continuously reinforced ceramic matrix composites made by tape casting to obtain uniform fiber spacing [5]. Photo-micrographic characterization to check consolidation in CMCs is again inadequate to provide reliable results.

In this paper, it will be demonstrated that ultrasonic NDE is a valuable tool for post-processing characterization and detection of microscopic defects arising during the fabrication of composites. Also, it will be shown that the technique can be reliably used to minimize the number of iterations required for optimization of the consolidation process. The application of two different ultrasonic techniques involving shear wave and longitudinal wave interrogations for evaluating the consolidation of advanced composites will be discussed. The examples provided here consist of ultrasonic evaluation of consolidation in various material systems including both metal matrix and ceramic matrix composites having various configurations (single fiber/ply etc.). Finally, in the case of ceramic matrix composites, the influence of residual stress, degree of wetting of the matrix to the fiber coating, and re-processing, on the degree of consolidation will be discussed.

2. Composite Samples

Two type of composite systems were used for this study. The first type was based on titanium matrices while the other was based on glass matrices.

2.1. Fabrication of Titanium Matrix Composites

Two types of samples were made:

(1) single fiber sample wherein the sample contained only one fiber,
(2) single layered multi-fiber sample wherein many fibers were placed in one ply of the sample.

2.1.1. *Single Fiber Composites*

These model composites consisting of an SCS-6 SiC fiber in a Ti-14Al-21Nb (wt. %) alloy matrix were fabricated in the form of 2 mm thick panels by diffusion bonding two matrix alloy sheets with a single fiber between them using two different processing conditions:

(1) Vacuum hot pressing at 925°C under 5.5 MPa pressure for 30 min followed by hot isostatic pressing (HIP'ing) at 1010°C under 100 MPa pressure for 2 hr (Panel A), and
(2) Vacuum hot pressing at 982°C under a pressure of 9.2 MPa for 30 min (Panel B).

2.1.2. *Single Ply Composites*

The single ply composites consisted of a layer of SCS-6 SiC fibers in a Ti-6Al-4V (wt. %) alloy matrix. These were also fabricated in the form of 2 mm thick panels by vacuum hot pressing at 954°C under a pressure of 9.2 MPa for 2 hr (Panel B).

2.2. Fabrication of Fiber Reinforced Ceramic Matrix Composites

The CMCs evaluated in this work consisted of SiC fiber reinforced glass matrix composites. A variety of composites based on glass matrices including the borosilicate glasses designated C, D, E, and F, and the fiber reinforcements SCS-6 and SCS-0 were investigated. The composites were processed by tape casting the glass powder into a green tape with a relative density of 50%. The green tapes were cut to size and laminated with fiber mats of the desired SiC fiber spacing (68 or 120 fibers per inch). The volume fraction of fibers in the composites was varied by altering the thickness of the green tape and using the two different fiber spacings. After lamination, the composites were inserted into a tube furnace and vacuum sintered at 730° C for one hour. The samples were then hot isostatically

pressed at 650° C for 30 min. with an applied pressure of 35 MPa to remove the residual porosity (~ 2%). The resulting samples were approximately 100 mm long by 2 cm wide with a thickness of 2 mm.

3. Ultrasonic Experimental Approach

The samples, both MMCs and CMCs, were ultrasonically imaged using two different techniques: (1) Shear wave interrogation and (2) Longitudinal wave interrogation. Figures 1 and 2 show schematics of these two techniques, respectively.

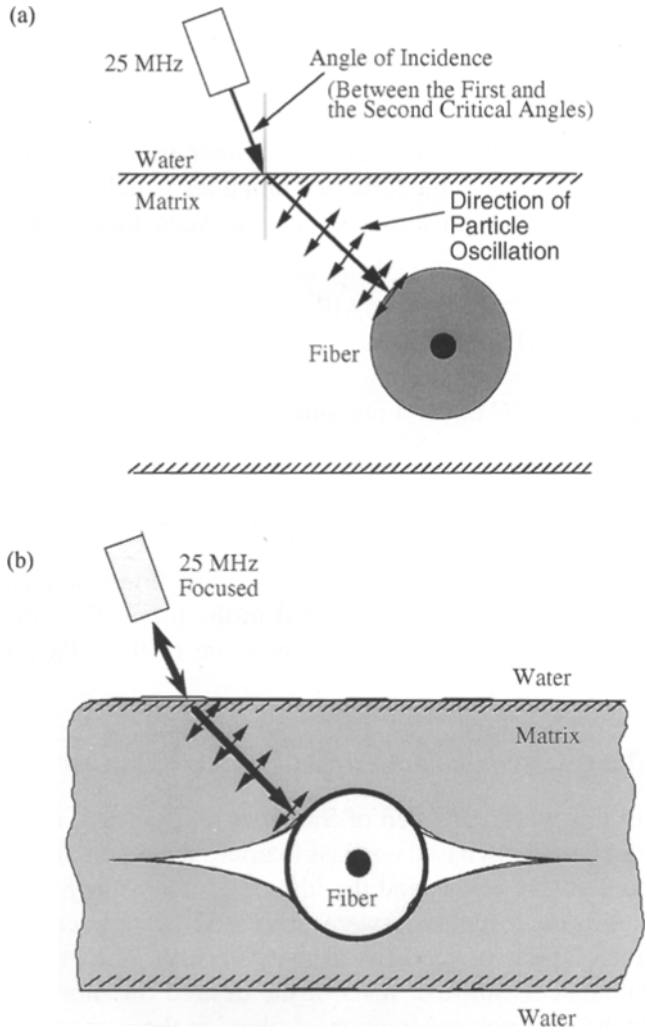

Figure 1. Schematic diagram of the transverse section of a continuously reinforced composite showing shear wave interrogation of a fiber embedded in the matrix: (a) Fully consolidated composite, and (b) Partially consolidated composite.

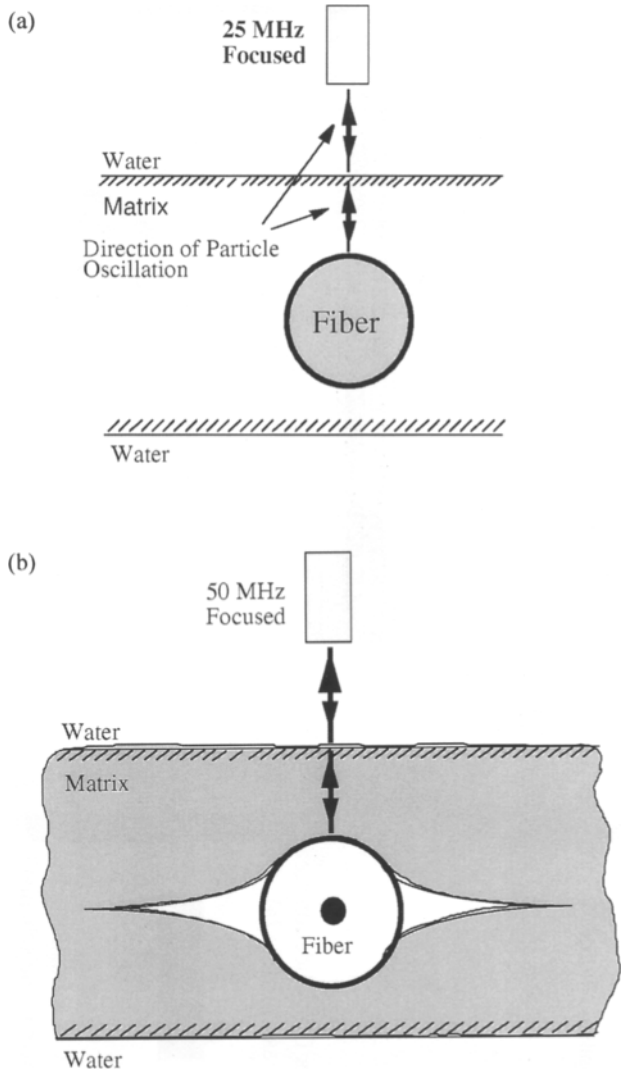

Figure 2. Schematic diagram of the transverse section of a continuously reinforced composite showing longitudinal wave interrogation of a fiber embedded in the matrix: (a) Fully consolidated composite, and (b) Partially consolidated composite.

In the shear wave technique, a 25 MHz focused transducer (6.3 mm diameter, 12.7 mm focal length) was used in the pulse-echo mode. The ultrasonic wave front was incident on the specimen. The angle of incidence was between the first and the second critical angles which are defined as the angles of incidence above which longitudinal and shear waves, respectively, will not propagate in the matrix material. As a result, only vertically polarized shear waves propagated (Figure 1) in the matrix with a refraction angle 'θ_S' (given by the Snell's

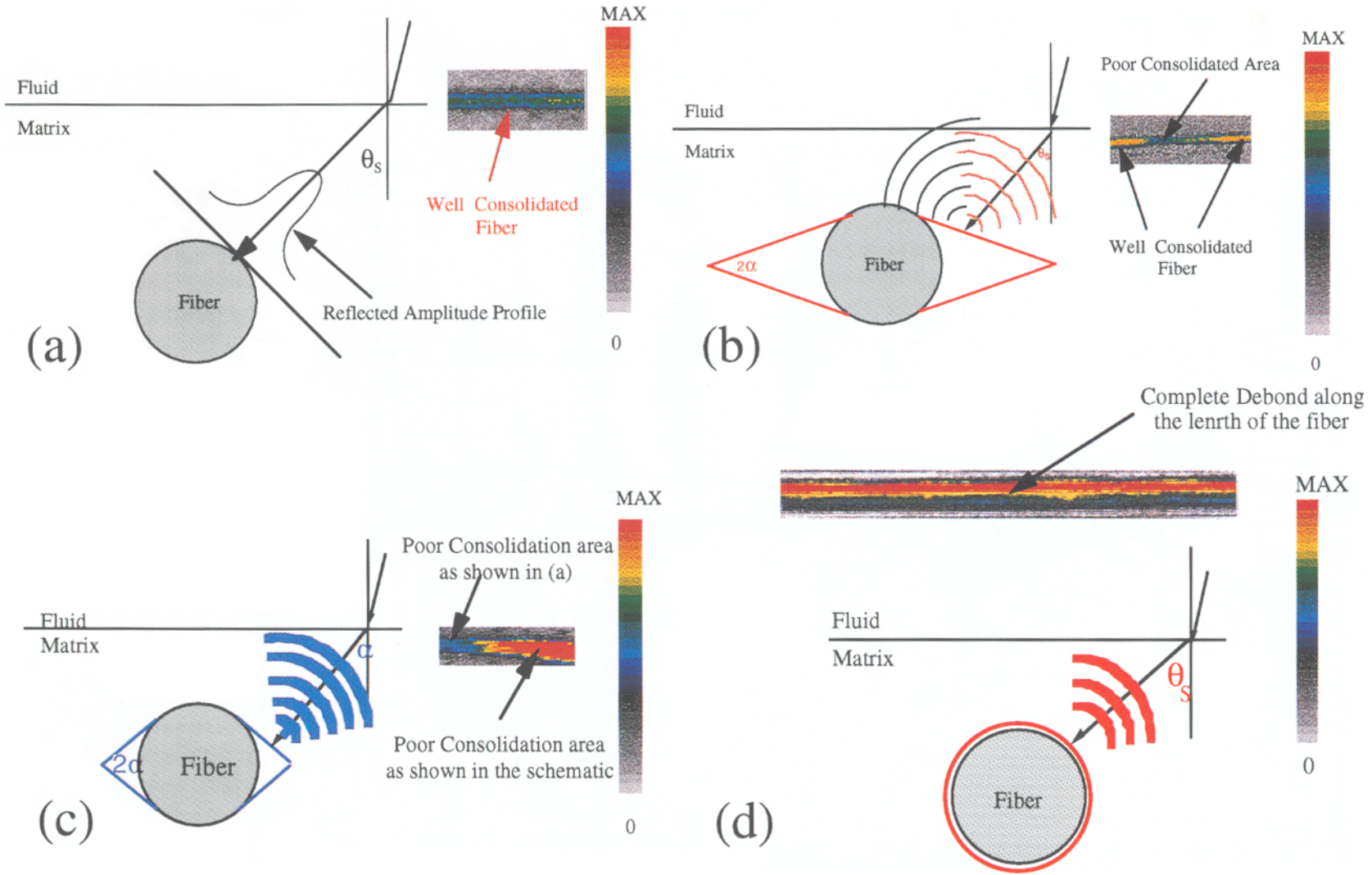
MAX
Fluid
Matrix
θ_S
Well Consolidated Fiber
Fiber
Reflected Amplitude Profile
0
(a)
MAX
Poor Consolidated Area
Fluid
Matrix
θ_S
2α
Fiber
Well Consolidated Fiber
0
(b)
Complete Debond along the lenrth of the fiber
MAX
Poor Consolidation area as shown in (a)
Fluid
Matrix
α
2α
Fiber
Poor Consolidation area as shown in the schematic
0
(c)
Fluid
Matrix
θ_S
Fiber
0
(d)

law [13], $\theta_S = \sin^{-1}\{(V_m/V_w)\theta_w\}$, where θ_w is the angle of incidence in water, V_m is the ultrasonic velocity in the matrix material, and V_w is the ultrasonic velocity in water. The ultrasonic images are formed when ultrasonic energy is reflected from the scattering cross-section of a reflector (cylindrical fiber) present in the path of wave propagation through a homogeneous medium (matrix). In the present application, the matrix may be assumed to be homogeneous since the wavelength of interrogation (130 μm) is large compared to the average grain size of the matrix ($< 10\,\mu$m).

The ultrasonic image of fibers with different degree of consolidation depends on the angle of incidence of the beam and the shape of the cross-section of the poor consolidation area. Figure 3a shows the reflected shear wave amplitude from a fiber in a fully densified composite. The reflected amplitude is maximum at the center of the fiber (which is a cylindrical reflector) and is gradually reduced as the transducer is scanning away from the center of the fiber. Figure 3b shows a general case of reflection of ultrasound from a fiber with poor consolidation where 'α' is the half angle of poor consolidation and is related to the shape of the defect. Here, the embedded reflector in the matrix is non cylindrical in shape as shown in Figure 3b. Therefore, the wave will be reflected away from the receiver and only a small part of the energy (which is incident on the region close to the top of the fiber) will come back to the transducer, thereby distorting the ultrasonic image of the fiber. Consequently, the image of the fiber will appear with a smaller diameter compared to a well consolidated fiber, and also the reflected ultrasonic amplitude will be lower (see color scale in Figure 3b). In Figure 3c, the half angle of poor consolidation is equal or close to the refraction angle of shear waves. In this case, a strong reflection is expected from the defect. The image of the fiber will appear much larger in diameter compared to a well consolidated fiber, and also the reflected ultrasonic amplitude will be maximum (total reflection). Figure 3d shows another type of defect which is a complete debond around the fiber. In this case the reflected ultrasonic amplitude will be maximum in the center of the fiber and will be reduced as the transducer is moving away from the center of the fiber. The image of the fiber will appear in this case with a diameter slightly larger than the well consolidated fiber and with maximum reflected amplitude.

In the longitudinal wave technique, a 50 MHz focused transducer (6.3 mm diameter, 25.4 mm focal length) was used in the pulse-echo mode and the wave

←*Figure 3.* (a) Reflected shear wave amplitude from a fiber in a fully densified composite. The reflected amplitude is maximum at the center of the fiber and is gradually reduced away from the center. (b) Reflection of ultrasound from a fiber with poor consolidation. The reflector embedded in the matrix is not cylindrical. The wave is reflected away from the receiver and only a small amount of energy comes back to the transducer. (c) Total reflection the case of $\alpha = \theta_S$. The fiber appears much larger in diameter compared to a well consolidated fiber. (d) Complete debond around the fiber. The reflected ultrasonic amplitude will be maximum in the center of the fiber.

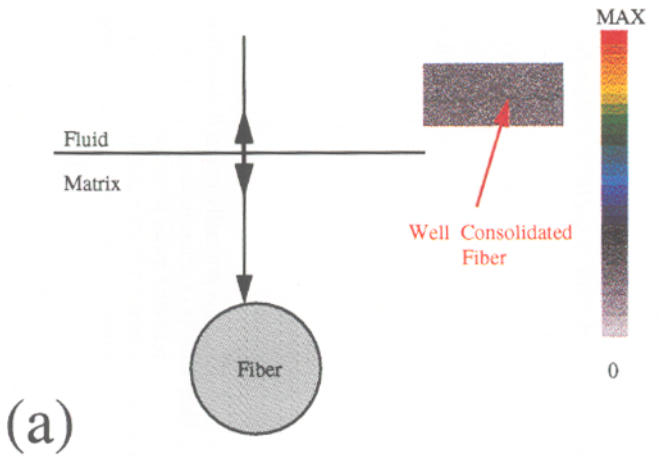
MAX
Fluid
Matrix
Well Consolidated Fiber
Fiber
0

(a)

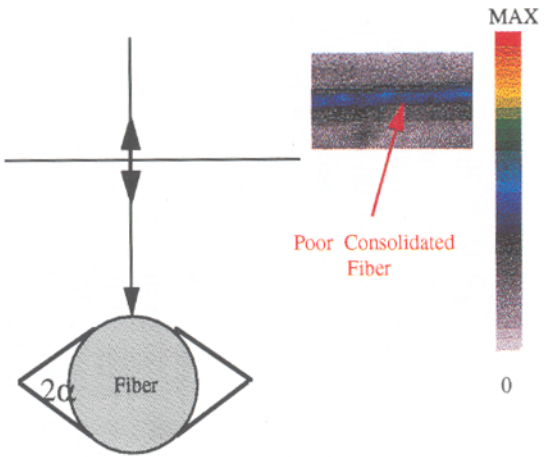
MAX
Poor Consolidated Fiber
2α
Fiber
0

(b)

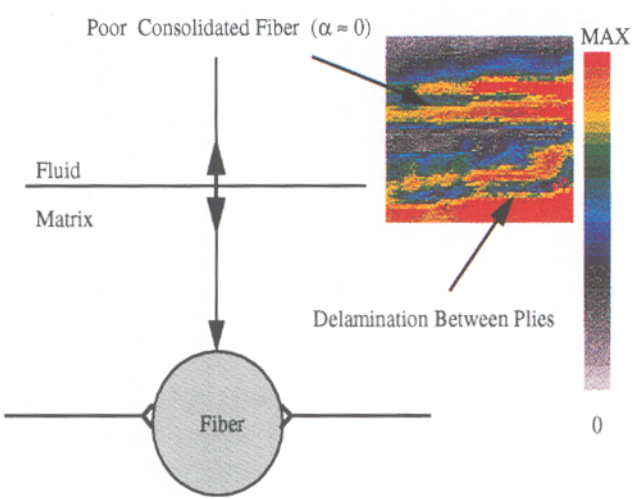
Poor Consolidated Fiber (α ≈ 0)
MAX
Fluid
Matrix
Delamination Between Plies
Fiber
0

(c)

front was incident normal to the specimen surface. Under this condition, a compressional wave propagates in the matrix and is reflected from the fiber back to the transducer. In the case of normal incidence longitudinal wave interrogation, and when a well consolidated fiber is imaged (Figure 4a), very small amount of signal will be reflected back to the transducer and the fiber will be barely visible. However, when a situation similar to the configuration in Figure 4b is presented, higher amplitude of the signal, compared to the case of Figure 4a, will be reflected back to the transducer and the image of the fiber will be as shown in the Figure 4b. Finally, when α is equal or close to 0° (implying delamination between plies), total reflection from the defect will be observed as shown in Figure 4c. A maximum reflected signal will also be observed in the case of a complete debonding around the fiber.

The reason for using a transducer of twice the frequency for the longitudinal wave technique compared to the shear wave technique is as follows. The wavelength of the wave propagating in the matrix is calculated by the simple expression, $\lambda = c_i/f$, where c_i is the velocity of the ultrasonic stress wave ($c_i = c_S$ or c_L for a shear or a longitudinal wave, respectively) and f is the frequency of interrogation. As an exemple, in the case of the Ti-14Al-21Nb matrix alloy, the velocity of the shear wave generated by the 25 MHz transducer was measured to be $c_S = 3209$ m/sec and, therefore, the wavelength was about 130 μm. The velocity of the longitudinal wave propagating in the same matrix was measured to be $c_L = 6489$ m/sec, which is approximately twice the shear wave velocity. Since the frequency of longitudinal wave interrogation was twice that of shear wave interrogation, the wavelength remained approximately the same (about 130 microns). Consequently, the two interrogation techniques can be directly compared based on the same resolution in terms of wavelength.

In both shear wave and longitudinal wave interrogation techniques, the image of the fiber was obtained by scanning the ultrasonic transducer along and across the fiber with an increment of 25 μm between signal acquisition points. At each point, the back-reflected ultrasound was software-gated for imaging [6]. The same ultrasonic techniques had also been used for evaluating the SiC glass matrix composites. In the case of a single-ply composite, because of the small spacing between fibers, a smaller angle of incidence was used (19°) to image the fibers without overlapping. The elastic properties of the matrix material (Ti-6Al-4V) used for the single-ply composites are close to the properties of the matrix material (Ti-14Al-21Nb) used for the single fiber composites, so the ultrasonic velocities in the matrix are practically the same and the wave-length of ultrasound remains the same (about 130 μm). The ultrasonic wave-length in the case of the ceramic matrix was also close (about 132 μm) to that in titanium composites.

←*Figure 4.* (a) Reflected longitudinal wave from a fiber in a fully densified composite. The fiber is barely visible. (b) Reflection of ultrasound from a fiber with poor consolidation. Bigger amount of signal, compared to case (a), will be reflected back to the transducer. (c) case of $\alpha \approx 0$. Total reflection from the defect.

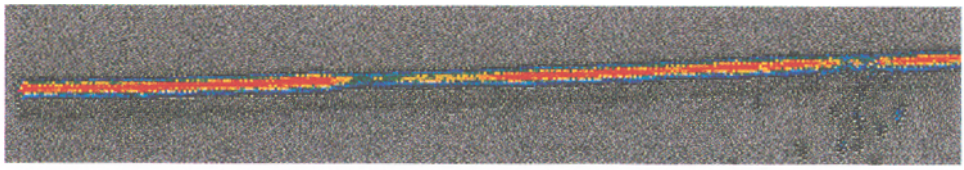

(a)

(b)

Figure 5. Ultrasonic image from Ti-14Al-21Nb/SiC sample which was consolidated by vacuum hot pressing + HIP'ing (Panel A) – (a) Shear wave interrogation with a wave front incidence of 24°, and (b) Longitudinal wave interrogation with normal incidence.

(a)

(b)

Figure 6. Ultrasonic images from Ti-14Al-21Nb/SiC single fiber composite (Panel B) using shear wave interrogation with different angles of wave front incidence: (a) 18° and (b) 24°.

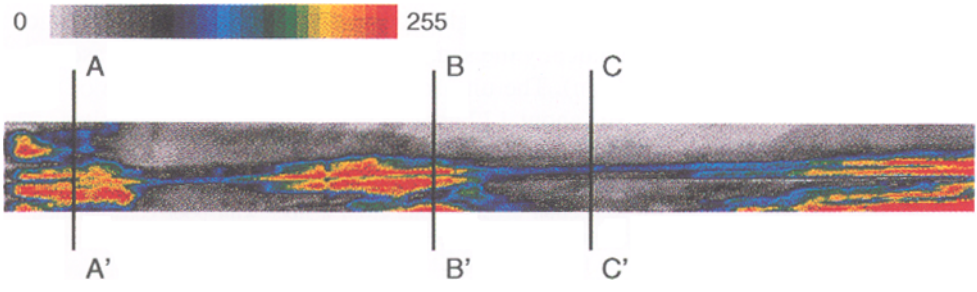

Figure 7. Ultrasonic image from Ti-14Al-21Nb/SiC single fiber composite (Panel B) using longitudinal wave interrogation. AA′, BB′, and CC′ indicate sections at which metallographic samples were examined.

In the case of metal matrix composites, the correlation between the ultrasonic image and the local microstructure was also studied by sectioning the samples normal to the fiber axis at several locations along the fiber. These sections were metallographically polished and examined by optical microscopy.

4. Results and Discussion

4.1. Titanium Matrix Composites

The ultrasonic images of the Ti-14Al-21Nb/SiC single fiber composite sample which was processed by vacuum hot pressing followed by HIP'ing (Panel A) are shown in Figure 5. Figure 5a corresponds to shear wave interrogation and shows uniform reflection along the fiber. Figure 5b shows the image resulting from longitudinal wave interrogation of this material and indicates that the reflected signal is uniformly weak along the length of the fiber.

Figure 6 shows two ultrasonic images of the composite sample consolidated by vacuum hot pressing alone (Panel B). The images were obtained by shear waves interrogation at two different angles of incidence. The use of different angles of incidence helps to determine the angle of the slope, α, of the matrix-void boundary and to map the extent and the shape of the consolidation defect. Also, it helps to detect variations of the shape of the void along the length of the fiber due to nonuniform consolidation. In the example shown in Figure 6, the two images of the fiber indicate significant variations in the reflected intensity along its length. The variation in amplitude of the images is because, varying angle of incidence varyies the refracted angle of shear waves, θ_S, thereby changing the difference between the angle of poor consolidation, α and θ_S. Further, because the defect has a variable slope and hence different 'effective scattering cross-section', the image of the fiber appears to possess a variable diameter along its length. As seen from Figure 6, this difference becomes smaller for an angle of incidence of 24° (Figure 6b) than for 18° (Figure 6a). Hence, for this particular case, α is closer to θ_S for an incidence of 24° than of 18°. Figure 6 also shows a nonuniformity of the defect in this panel. The nonuniformity in this panel is also evident from the image obtained by longitudinal wave interrogation (Figure 7).

An optical micrograph of a cross section of the composite panel A is shown in Figure 8. This micrograph shows that the consolidation of the matrix around the fiber is complete in this composite. This result was typical of the various cross sections examined, suggesting that the consolidation occurred uniformly within the panel A. Figure 9 shows optical micrographs of the composite panel B corresponding to the sections AA′, BB′ and CC′ which are indicated in Figure 7. It is clear from these micrographs that the bonding of the matrix alloy sheets is incomplete around the fiber. Further, there is a considerable variation in the degree of bonding of the matrix along the length of the fiber (Figure 9).

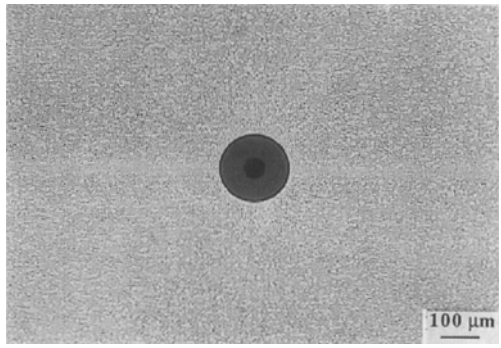

Figure 8. Optical micrograph of Ti-14Al-21Nb/SiC single fiber composite (Panel A) sample showing good consolidation.

A good correlation is found between the micrographs of the composite panels and the observed ultrasonic images. These results show that the diffusion-bonding conditions used for processing of panel B did not lead to complete consolidation, whereas panel A was fully consolidated. These results are in general agreement with previous observations dealing with the sequence of events during the consolidation of such composites by the foil-fiber-foil method [7–8]. When the foil-fiber-foil preform is subjected to elevated temperature under pressure, the process begins with the indentation of matrix alloy foils by the fibers and is followed by matrix creep, leading to diffusion- bonding between the foils. At the end of this stage, two large pores remain on opposite sides of each fiber along the bond plane of the foils due to lower local stresses [7–11] as observed in Figure 9. The composite is fully consolidated when these remnant voids near the fibers are eliminated (Figure 8). The present results also indicate that consolidation can occur nonuniformly along the length of the fiber (Figure 9). Clearly, metallographic characterization alone is tedious under such conditions and other techniques such as ultrasonic NDE will be very useful.

In contrast to the images of poor consolidation described before, images of well consolidated fibers show a different pattern. In the case of shear wave interrogation, mode-converted shear waves propagate through the matrix and are back-scattered from the fiber (Figure 1). When the matrix is completely consolidated around the fiber, the maximum of the reflected signal occurs when the polarized shear waves propagating in the matrix are incident perpendicular to the circumference of the cylindrical fiber as indicated in Figure 3a. It should be noted that the maximum of the received energy corresponds to the main lobe of the Bessel function which is the theoretical response of a cylindrical reflector embedded in a medium [12]. Thus, a well-consolidated sample will provide an image as shown in Figure 5a. In the case of longitudinal wave interrogation, compressional waves are incident normal to the surface of the panel specimen as

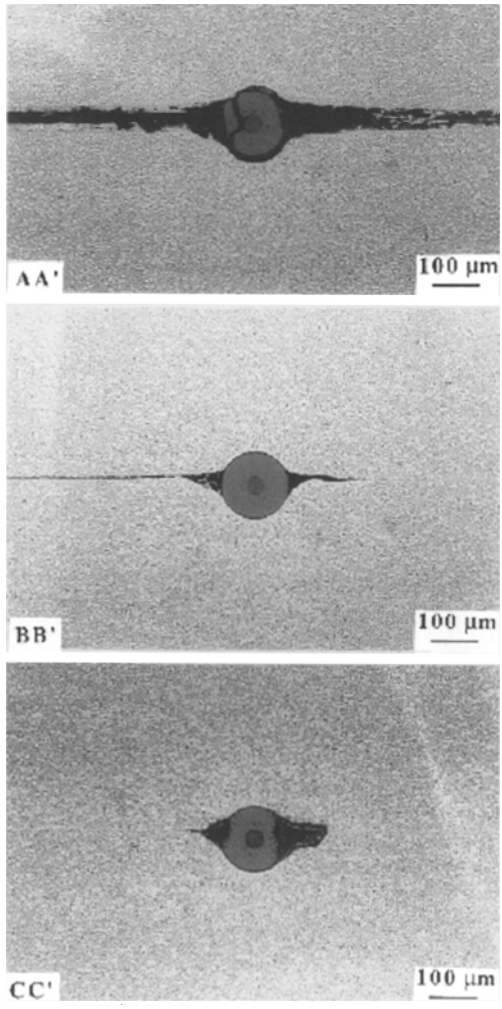

Figure 9. Optical micrographs of vacuum hot pressed Ti-14Al-21NB/SiC (Panel B) sample showing poor consolidation at sections (a) AA′ (b) BB′, and (c) CC′.

well as the foil-foil interface as shown in Figure 2. When the composite is fully consolidated, longitudinal waves are much less sensitive to various fiber/matrix interfacial conditions as compared to shear waves [14] and the reflected amplitude does not show any wide fluctuations (Figure 5b).

Although these results were obtained from a model composite containing a single fiber, these ultrasonic techniques are equally applicable for studying the consolidation of real composites containing a high volume fraction of fibers. Figure 10 shows an image obtained by shear wave interrogation of a Ti-6Al-4V/SiC single-ply composite specimen. The non uniform reflection along a number of fibers is evident, implying global poor consolidation. Metallographic examination

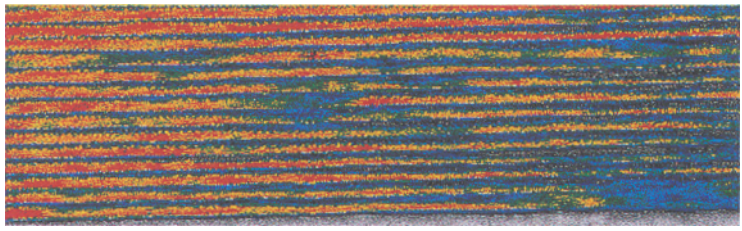

Figure 10. Shear Wave Interrogation of a Ti-6Al-4V/SiC Single-ply Composite Showing Areas of Poor Consolidation.

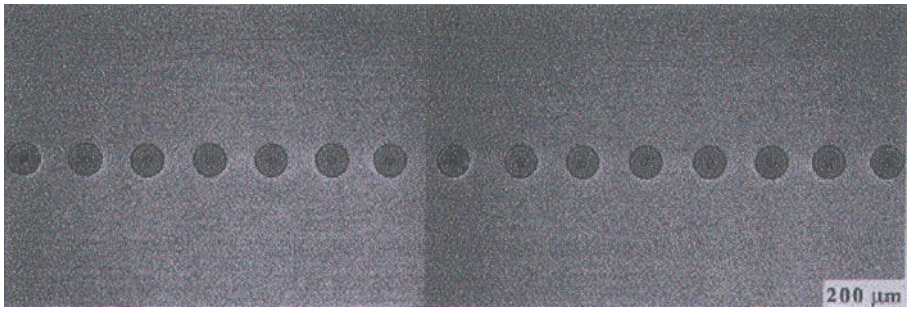

Figure 11. Metallography of Section from a Uniform Region Showing Good Consolidation.

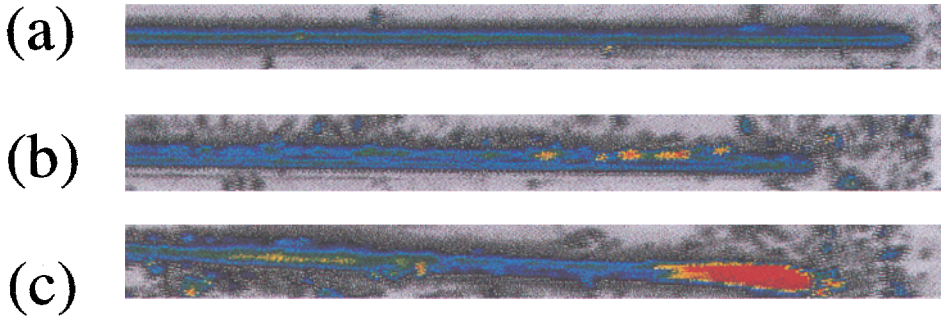

Figure 12. (a) Glass-F/SCS-6 composite showing good consolidation. (b) Glass-F/SCS-6 composite showing poor consolidation (c) Glass-F/SCS-0 composite showing poor consolidation Porosity in the matrix can be observed in all three composites.

of sections from the uniform region of a sample confirmed good consolidation as shown in Figure 11. Metallographic sections corresponding to the regions of nonuniform reflection revealed incomplete consolidation similar to the results shown in Figure 9. With regard to the evaluation of composites containing a high volume fraction of fibers, it should be noted that the shear wave technique is useful for studying the outermost layer of fibers while the longitudinal wave interrogation is more suited for detecting macroscopic defects.

In addition to the studies of composite consolidation, these NDE methods are very useful for the detection of fiber fractures and fiber-matrix interfacial debonding in continuously reinforced metal matrix composites [15]. Further details on the ultrasonic evaluation of consolidation in MMCs can be found in literature [16, 17].

4.2. Ceramic Matrix Composites

Lack of consolidation in CMCs due to processing conditions can be detected using ultrasound as shown below. Figure 12 shows the ultrasonic images of three single fiber ceramic matrix composites made with glass-F matrix. The fibers were imaged using the shear wave interrogation technique. Figure 12a shows the a glass-F/SCS-6 single fiber composite with relatively uniform reflection along the fiber, implying a good consolidation along the length of the fiber. Figure 12b shows another sample (glass-F/SCS-6), but with poor consolidation along the length of the fiber. Figure 12c shows a glass-F/SCS-0 single fiber composite with poor consolidation along the length of the fiber. Here (Figure 12c) there is a variation in the degree and angle of consolidation of the matrix along the length of the fiber.

Partial debonding due to the state of radial residual stresses at the interface can also be detected using ultrasonic NDE as discussed below. Figure 13 shows three single-ply samples made with SCS-6 fibers and three different borosilicate glass matrices having slightly different chemical composition so that their coefficients of thermal expansion vary while their elastic properties remain similar [18]. The fibers were imaged using the shear wave interrogation technique. Figure 13a shows a glass-D/SCS-6 single-ply composite with some tensile radial residual stress (σ_r), because of the thermal expansion coefficient mismatch between fiber and matrix. Therefore, regions of localized debonding are observed. Figure 13b shows a glass-C/SCS-6 single-ply composite with a substantial tensile radial residual stress. Extended debond was observed in this case. Figure 13c shows a glass-E/SCS-6 single-ply composite with almost zero radial residual stress. Here, a good consolidation was observed along the length of the fibers.

The ultrasonic technique has been also used to evaluate the consolidation of multi-fiber CMCs. Figure 14 shows two single-ply samples made with glass-E matrix and two different types of fibers. Figure 14a shows a glass-E/Sigma single-ply composite imaged using the shear wave interrogation technique. The

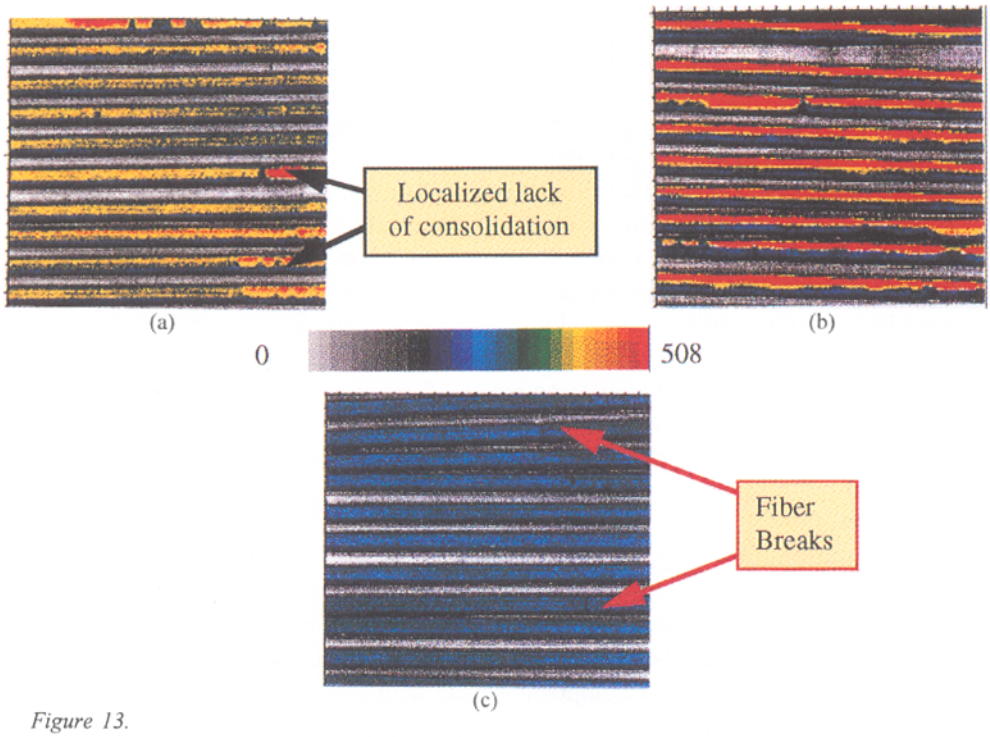

Figure 13.

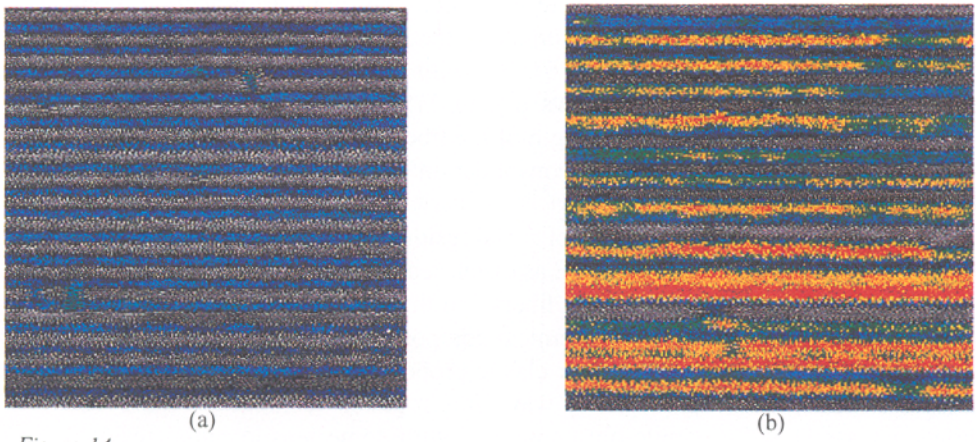

Figure 14.

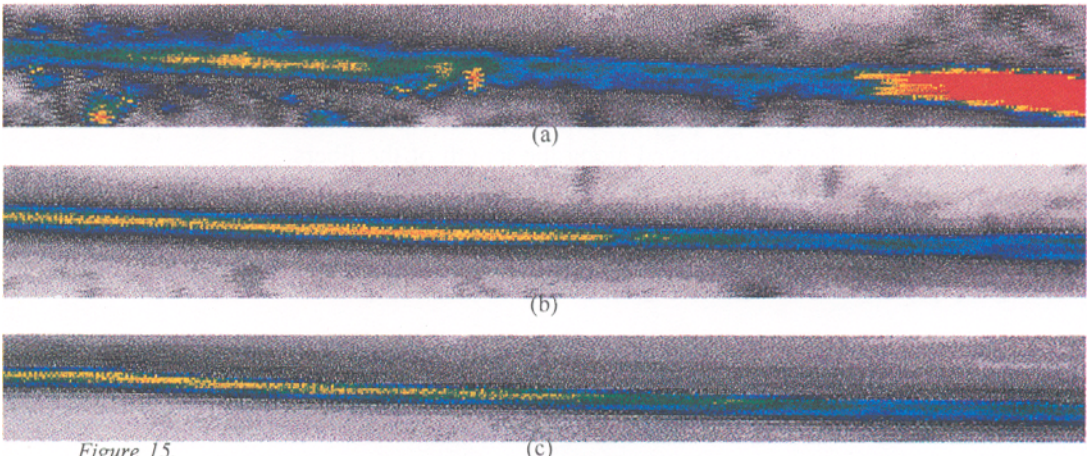

Figure 15.

borosilicateglass strongly wets the TiB_2 coating of the SIGMA fiber, therefore, the consolidation along the fiber was good [18]. Figure 14b shows a glass-E/SCS-6 single-ply composite. The glass weakly wets the carbon coating of the SCS-6 fiber [18], hence, global lack of consolidation was seen in this case.

The lack of consolidation of CMCs can be alleviated if the processing parameters are adjusted with information from ultrasonic evaluation of the samples as discussed in this paragraph. A glass-F/SCS-6 single fiber composite was used for this study. The composite was processed using a single binder burnout and sinter schedule: the sample was vacuum sintered for one hour at 730° C. The furnace was then backfilled with argon while maintaining 730° C for 20 min. The sample was then cooled to room at 5° C/min. Next the sample was HIP'd at 650° C for 30 min with an applied pressure of 34.5 MPa to remove the residual porosity. Figure 15a shows an ultrasonic SBR image of the sample after processing. From Figure 15a it can be seen that the sample appears to be poorly consolidated. Taking advantage of the use of a nondestructive technique to evaluate the consolidation of the composite, it was decided to reprocess the specimen and evaluate it again with the SBR technique. The sample was re-HIP'd at 700° C for 30 min with the same applied pressure of 34.5 MPa. The ultrasonic image of the re-HIP'd sample, Figure 15b, shows an great improvement in both the consolidation around the fiber and a significant reduction of porosity in the matrix. Finally, the sample was HIP'd for a third time at 730° C for 30 min with the same applied pressure. The ultrasonic image this time showed uniform consolidation along the fiber (Figure 15c). Also, the porosity in the matrix was eliminated. The reason for the improvement in consolidation and the reduction of the porosity shown in Figure 15 is that, by increasing the processing temperature, the viscosity of the glass decreases significantly. For example, if the temperature increases by 50° C (i.e. from 650° C to 700° C), the viscosity of the glass decreases by a factor of

↖ *Figure 13.* (a) Single ply glass-D/SCS-6 composite with localized areas of poor consolidation (σ_T = 6.5 MPa tensile). Here, red color indicates complete lack of consolidation. (b) Single ply glass-C/SCS-6 composite global lack of consolidation (σ_T = 13.6 MPa tensile). (c) Single ply glass-E/SCS-6 composite with Good Consolidation (σ_T is almost zero).

↖ *Figure 14.* (a) Single ply glass E/Sigma composite showing Good Consolidation. (b) Single ply glass E/SCS-6 composite showing Poor Consolidation.

←*Figure 15.* Nondestructive Evaluation of Consolidation in a Glass-F/SCS-6 Single Fiber Composite Using SBR Technique. (a) The Processed Composite Shows bad Consolidation along the Fiber and Substantial Matrix Porosity. (b) The Same Sample Showing Improvement in both the Consolidation and Porosity after Reprocessing by Increasing the Previous Processing Temperature. (c) The Sample Shows Good Consolidation and Absence of Matrix Porosity after being Processed for a Third Time by Further Increasing the Previous Processing Temperature.

$\approx$ 10. By decreasing the viscosity it is easier for the glass to densify around the fiber forming a well consolidated composite with porosity free matrix. Since small changes in temperature may result in big changes of the viscosity of a glass, due to the logarithmic relationship between temperature and viscosity, it is difficult in many cases to predict a processing temperature at which the composite is well consolidated while minimizing the thermal damage to the fibers. It is shown through this work that ultrasonic NDE may be useful in the evaluation of post-processed composites to provide important information thereby helping to refine the processing parameters of composite materials.

5. Summary

In this paper, a nondestructive ultrasonic approach has been described to evaluate the interfacial defects induced during processing in both metal matrix and ceramic matrix composites. Two different modes of ultrasonic interrogation have been presented, one based on shear waves and the other based on longitudinal waves. Application of the technique to a variety of interface defect manifestations has been discussed in details. Also, the effect of radial residual stresses on the integrity of the fiber-matrix interface has been investigated in the case of different glass matrix composites with various residual stresses ranging from compressive to tensile. Finally, the usefulness of the technique for the optimization of the processing of ceramic matrix composites has been shown.

References

1. Johnson, W. S., 'Screening of Metal Matrix Composites Using Ultrasonic C-Scans', *J. Comp. Tech, & Res.*, 1989, 31–34.
2. Liaw, P. K. *et al.*, 'Determining Material Properties of Metal-Matrix Composites by NDE', *J. Mat.* 44(10), 1992, 36–40.
3. Bampton, C. C., Graves, J. A., Newell, K. J. and Lorenz, R. H., 'Process Modeling for Titanium Aluminide Matrix Composites,' in F. H. Froes and I. L. Caplan (ed.), *Titanium '92: Science and Technology*, TMS, Warrendale, PA, 1993.
4. Larsen, J. M., Revelos, W. C. and Gambone, M. L., in D. B. Miracle, D. L. Anton and J. A. Graves (eds), *MRS Symposium Proceedings*, Vol. 273, Intermetallic Composites II, 1992, pp. 3–16.
5. Gustafson, C. and Dutton, R. E., 'The Effect of Fiber Coating upon the Densification of Sintered Borosilicate Glass/SiC Fiber Composites', in *Proceedings of the International Conference on Composites Engineering (ICCE/1)*, New Orleans, 1994, pp. 139–140.
6. Buynak, C. F., Moran, T. J. and Martin, R. W., 'Delamination and Crack Imaging in Graphite-Epoxy Composites', *Mat. Eval.* **47**, April 1989, 438–447.
7. Guo, Z. X. and Derby, B., in A. J. Paul, S. N. Dwiveti and F. R. Dax (eds), *Concurrent Engineering Approach to Materials Processing*, The Minerals, Metals and Materials Society, Warrendale, PA, 1992.
8. Nicolaou, P. D., Piehler, H. R. and Saigal, S., in A. J. Paul, S. N. Dwiveti and F. R. Dax (eds), *Concurrent Engineering Approach to Materials Processing*, The Minerals, Metals and Materials Society, Warrendale, PA, 1992.
9. Nicolaou, P. D., Piehler, H. R. and Saigal, S., 'Experimental and Finite Element Analytical Guidelines for Fabricating Continuous Fiber (SCS-6) Metal Matrix (Ti-6Al-4V) Composites via the Foil/Fiber/Foil Technique', to appear in *J. Comp. Mat.* **25**, 1995.

10. Nicolaou, P. D., Piehler, H. R. and Kuhni, M. A., 'Fabrication of Ti-6Al-4V Matrix, SCS-6 Fiber Composites by Hot Pressing Using the Foil/Fiber/Foil Technique', in K. Upadhya (ed.), *Developments in Ceramic and Metal-Matrix Composites*, The Minerals, Metals, and Materials Society, Warrendale, PA, 1991, pp. 37–47.
11. Nicolaou, P. D., Piehler, H. R. and Saigal, S., 'Process Parameter Selection for the Consolidation of Continuous Fiber Reinforced Composites Using Finite Element Simulations', *Int. J. Mech. Sci.* **37**, 1995, 669–690.
12. Schuetz, L. S. and Neubauer, W. G., 'Acoustic Reflection from Cylinders – Nonabsorbing and Absorbing', *J. Acoust. Soc. Am.* **62**, 1977, 513–517.
13. Krautkrämer, J. and Krautkrämer, H., *Ultrasonic Testing of Materials*, Springer-Verlag, New York, 1990.
14. Matikas, T. E. and Karpur, P., 'Ultrasonic Reflectivity Technique for the Characterization of Fiber-Matrix Interface in Metal Matrix Composites', *J. Appl. Phys.* **74**(1), 1993, 228–236.
15. Karpur, P., Matikas, T. E. and Krishnamurthy, S., 'Matrix-Fiber Interface Characterization in Metal Matrix Composites Using Ultrasonic Imaging of Fiber Fragmentation', in *Proceedings of the American Society for Composites 7th Technical Conference*, Pennsylvania State University, University Park, PA, 1992, pp. 420–427.
16. Krishnamurthy, S., Matikas, T. E., Karpur, P. and Miracle, D. B., 'Evaluation of the Processing of Fiber-Reinforced Metal Matrix Composites Using Ultrasonic Methods', to appear in *J. Comp. Sci. Tech.*, 1995.
17. Matikas, T. E. and Karpur, P., 'Ultrasonic Nondestructive Evaluation as a Tool for the Development of Aerospace Structural Ceramic Composites', NATO/AGARD 76th Meeting of the Structures and Meterials Panel, Antalya, Turkey, 1993.
18. Matikas, T. E. and Karpur, P., 'Micro-mechanics Approach to Characterize Interfaces in Metal and Ceramic Matrix Composites', in D. O. Thompson and D. E. Chimenti (eds), *20th Annual Review of Progress in Quantitative Nondestructive Evaluation* **13B**, Plenum, Bruswick, Maine, 1993, pp. 1477–1484.
19. Pagano, N. J., Dutton, R. E., Kim, R. Y., Karpur, P., Matikas, T. E. and Gustafson, C., 'Influence of The Fiber-Matrix Interface on the Micro-Cracking in Unidirectional Glass Matrix Composites', in *Proceedings of the International Conference on Composites Engineering (ICCE/1)*, New Orleans, 1994, pp. 387–388.